

Kinetic studies on the thermal dissociation of β -cyclodextrin–benzyl alcohol inclusion complex

Ning Zhang ^a, Jing-Hua Li ^{a,*}, Qing-Tang Cheng ^a and Ming-Wei Zhu ^b

^a Department of Chemistry, Henan Normal University, Xinxiang 453002
(People's Republic of China)

^b Department of Biology, Henan Normal University, Xinxiang 453002
(People's Republic of China)

(Received 26 May 1993; accepted 5 July 1993)

Abstract

The stability of β -CD · C₇H₈O · 5H₂O was investigated using TG and DSC. The weight loss takes place in three stages: the dehydration occurs at 47–110°C; the dissociation of β -CD · C₇H₈O occurs at 200–250°C; and the decomposition of β -CD begins at 270°C. The kinetics of the dehydration of β -CD · C₇H₈O · 5H₂O and the dissociation of β -CD · C₇H₈O in a dry nitrogen flow were studied by means of thermogravimetry, both at constant temperature and with linearly increasing temperatures. The dehydration of β -CD · C₇H₈O · 5H₂O is dominated by a three-dimensional phase boundary reaction, R₃. The activation energy E is 101.75 kJ mol⁻¹. The pre-exponential factor A is 9.502×10^{10} min⁻¹. The dissociation of β -CD · C₇H₈O is affected by a two-dimensional diffusion process, D₂. The activation energy E is 158 kJ mol⁻¹. The pre-exponential factor A is 3.3×10^{14} min⁻¹. Scanning electron microscope observation and crystal structure analysis are in good agreement with the results obtained from thermogravimetry.

INTRODUCTION

β -Cyclodextrin is an annular molecule composed of seven glucose units linked by 1,4-glucosidic bonds [1]. Due to its annular structure, as a host molecule it is able to form inclusion complexes with a great variety of guest molecules. Its inclusion function can change the stability of the guest molecules. Toxicity experiments show that β -CD can be absorbed as a carbohydrate by animal and human bodies [2]. Inclusion complexes of β -CD with many organic compounds have been successfully utilized in the pharmaceutical and food industries [3–5]. Stability and kinetic studies on inclusion complexes in water have also been reported [6, 7]. The stability and kinetic mechanisms of the thermal decomposition of inclusion complexes in the solid state present interesting problems in industrial applica-

* Corresponding author.

tions. In this paper, the stability of β -CD \cdot C₇H₈O \cdot 5H₂O, the kinetics of its dehydration, and the dissociation of β -CD \cdot C₇H₈O were investigated in the solid state.

So far, many methods for identification of the kinetic mechanisms of solid-state reactions have been reported, but the kinetic parameters and the mechanisms reported by different authors are often different. This is because many methods rely on judging the linearity of one logarithmic form against another. In many cases, the linearity is comparable for different mechanism functions. Thus, it is difficult to distinguish precisely the mechanisms. We believe that it is not sufficient to identify a kinetic mechanism by only one method. Correct results can only be obtained by combination of two or three methods. However, because solid-state reactions are very dependent on crystal structure, the results obtained by thermogravimetry should be identified using other techniques [8–10], such as X-ray diffraction, microscopy, etc. Therefore, we judge the kinetic mechanism not only by Sharp's standard curve method at constant temperature [11] but also by Criado's standard curve method using temperature-programmed heating [12]. The results are satisfactory and in good agreement with crystal structure analysis.

EXPERIMENTAL

Preparation of the sample

β -CD (purchased from Beijing University) and benzyl alcohol (reagent grade) were dissolved in a 1:1 molar ratio in hot water. The solution was cooled down to room temperature for 24 h and then filtered. The sheet-like prismatic crystals were air-dried, ground and sieved to less than 75 mesh. The composition was identified by TG analysis as β -CD \cdot C₇H₈O \cdot 5.1H₂O. When 5.0 g of β -CD were dissolved in 20 ml of hot water using the same process, β -CD \cdot 10.8H₂O was obtained.

Apparatus and measurements

Thermogravimetric analysis was performed on a WRT-1 microbalance (Shanghai Balancing Instruments Factory). The analytical parameters were: sample mass, about 15 mg; heating rate, 1.2, 2.5, 5, 10°C min⁻¹; chart speed, 4 mm min⁻¹; atmosphere, dynamic dried nitrogen 30 ml min⁻¹; sample holder, aluminium crucible.

Differential scanning calorimetry was carried out on a CDR-1 differential scanning calorimeter (Shanghai Balancing Instruments Factory). The experimental conditions were: heating rate, 5°C min⁻¹; sample mass, about 5 mg; atmosphere, static air; reference material, Al₂O₃.

The structural changes in the thermal decomposition were observed on a Model 1000B scanning electron microscope (Amray Co., USA).

All the thermogravimetric data (α , 0.1–0.9) were analysed on an IBM PC-1500 microcomputer. A linear regression program was used.

RESULTS AND DISCUSSION

The stability of the inclusion complexes

Figure 1 shows the TG and DSC curves of β -CD \cdot 10.8H₂O and β -CD \cdot C₇H₈O \cdot 5.1H₂O.

The TG curve of β -CD \cdot 10.8H₂O indicates that all the constitutional water is released at 47–110°C with a weight loss of 13.85%. At 270°C, further weight loss indicates the decomposition of β -CD. The endothermic peaks at 85 and 300°C in the DSC curve are consistent with the dehydration of β -CD \cdot 10.8H₂O and the decomposition of β -CD on the TG curve, respectively.

Differing from β -CD \cdot 10.8H₂O, β -CD \cdot C₇H₈O \cdot 5.1H₂O has a 7.54% weight loss at 200–250°C as well as a 6.51% weight loss at 50–110°C, and a larger weight loss at 270°C. The DSC curve has an additional low endothermic peak at 230°C compared with β -CD \cdot 10.8H₂O. The extra weight loss (or endothermic peak) at 200–250°C corresponds to the escape

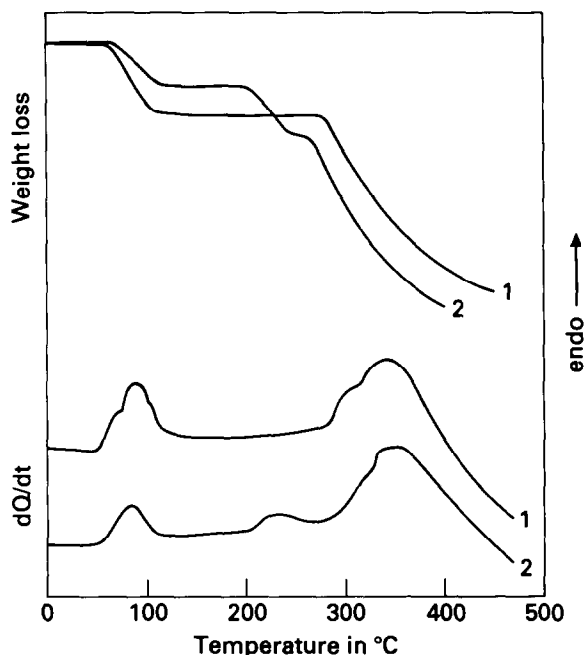


Fig. 1. TG and DSC heating curves of β -CD C₇H₈O 5.1H₂O and β -CD \cdot 10.8H₂O, heating rate = 5°C min⁻¹: curves 1, β -CD \cdot 10.8H₂O; curves 2, β -CD \cdot C₇H₈O \cdot 5.1H₂O.

of benzyl alcohol from the β -CD cavity. The dissociation of β -CD \cdot C₇H₈O above 200°C shows that β -CD can form a stable inclusion complex with benzyl alcohol.

The identification of the kinetic mechanism

The kinetics of a solid-state decomposition reaction can be represented by the general equation

$$\frac{d\alpha}{dt} = kf(\alpha) \quad (1)$$

or

$$g(\alpha) = kt \quad (2)$$

where α is the fraction of weight loss at the reaction time t , k is the rate constant, and $f(\alpha)$ and $g(\alpha)$ are functions describing the reaction mechanism. Typical theoretical model functions for solid-state reactions are shown in Table 1.

Isothermal studies

Figure 2 shows a plot of the fraction of weight loss α , against time t of the reaction at constant temperature.

The kinetic mechanism of the weight loss process can be judged by the linearity of the $g(\alpha)$ against time t plot. Taking the dissociation of β -CD \cdot C₇H₈O at 220°C as an example, Table 2 lists the linear regression results of $g(\alpha)$ versus t .

The results show that in many cases the correlation coefficient r is very near to unity, and the covariance δ is low. For the dissociation of β -CD \cdot C₇H₈O, mechanisms D₂, D₄ and A₁ have almost equally good

TABLE 1
Typical model functions $g(\alpha)$ for solid-state reactions

Symbol	$g(\alpha)$	Type
D ₁	α^2	One-dimensional diffusion
D ₂	$\alpha + (1 - \alpha)[\ln(1 - \alpha)]$	Two-dimensional diffusion
D ₃	$[1 - (1 - \alpha)^{1/3}]^2$	Three-dimensional diffusion (Jander function)
D ₄	$1 - 2/3\alpha - (1 - \alpha)^{2/3}$	Three-dimensional diffusion (G-B function)
Au	$\ln[\alpha/(1 - \alpha)]$	Autocatalytic reaction (P-T function)
R _{<i>n</i>}		Phase-boundary reaction ($n = 1, 2, 3$: one-, two-, and three-dimensional)
A _{<i>m</i>}	$[1 - \ln(1 - \alpha)]^{1/m}$	Random nucleation and subsequent growth (Avrami-Erofeyev function)

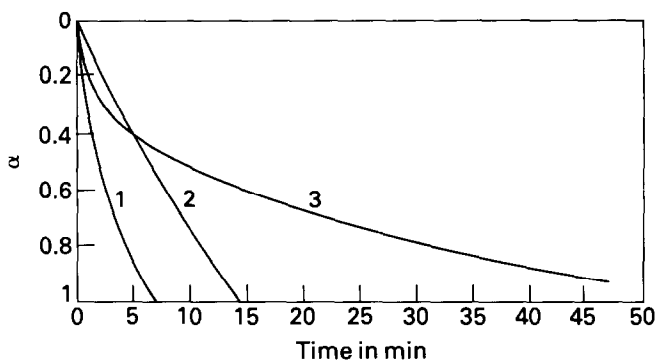


Fig. 2. Isothermal weight loss curves: 1, dehydration of β -CD \cdot C₇H₈O \cdot 5.1H₂O at 85°C; 2, evaporation of benzy alcohol at 110°C; 3, dissociation of β -CD \cdot C₇H₈O at 220°C.

linearity. So it is difficult to judge the kinetic mechanism on the linearity alone.

The linear regression analyses for the dehydration of β -CD \cdot C₇H₈O \cdot 5.1H₂O and the evaporation of C₇H₈O give similar results. R₂, R₃ and A₂ are suitable mechanisms for the dehydration of β -CD \cdot C₇H₈O \cdot 5.1H₂O. R₁, A₃ and A₄ are suitable for the evaporation of C₇H₈O.

In order to select one of these mechanisms, Sharp's standard curves method at constant temperature was considered. In eqn. (2), let $\alpha = 0.5$

$$g(0.5) = kt_{0.5} \quad (3)$$

where $t_{0.5}$ is the time at $\alpha = 0.5$. Combining eqns. (2) and (3)

$$\frac{g(\alpha)}{g(0.5)} = \frac{t}{t_{0.5}} \quad (4)$$

TABLE 2

The results of the linear regression fit to the dissociation of β -CD \cdot C₇H₈O at 220°C

$g(\alpha)$	k/min^{-1} ^a	r ^b	δ ^c	$g(\alpha)$	k/min^{-1} ^a	r ^b	δ ^c
D ₁	1.968×10^{-2}	0.9958	2.422	R ₂	1.422×10^{-2}	0.9867	1.749
D ₂	1.496×10^{-2}	0.9997	1.841	R ₁	1.094×10^{-2}	0.9913	1.347
D ₃	5.416×10^{-3}	0.9962	0.6663	A ₁	4.424×10^{-2}	0.9974	5.443
D ₄	3.923×10^{-3}	0.9994	0.4827	A ₂	2.475×10^{-2}	0.9799	3.045
Au	8.435×10^{-2}	0.9667	10.377	A ₃	1.727×10^{-2}	0.9685	2.125
R ₁	1.882×10^{-2}	0.9665	2.316	A ₄	1.353×10^{-2}	0.9641	1.664

^a Rate constant. ^b Correlation coefficient. ^c Covariance.

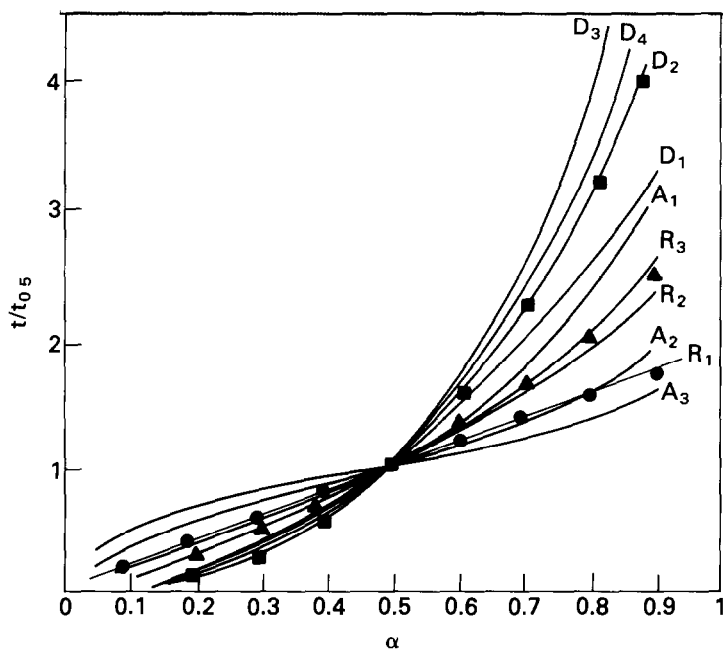


Fig. 3. Standard curves at constant temperature for ●, the evaporation of C_7H_8O at $110^\circ C$; ▲, the dehydration of $\beta\text{-CD} \cdot C_7H_8O \cdot 5H_2O$ at $85^\circ C$; ■, the dissociation of $\beta\text{-CD} \cdot C_7H_8O$ at $220^\circ C$.

For a definite mechanism function, the plots of $g(\alpha)/g(0.5)$ against α give standard curves and plots of $t/t_{0.5}$ against α give experimental curves. The correct function can be judged by the degree of coincidence with the experimental curves.

The standard curves of various model functions are shown in Fig. 3. The experimental points for the dissociation of $\beta\text{-CD} \cdot C_7H_8O$ at $220^\circ C$ clearly fall on curve D_2 , and the experimental points for the dehydration of $\beta\text{-CD} \cdot C_7H_8O \cdot 5H_2O$ and the evaporation of C_7H_8O fall on curves R_3 and R_1 , respectively.

Therefore, from the linearity and the standard curves method, the evaporation of C_7H_8O is dominated by R_1 , the dehydration of $\beta\text{-CD} \cdot C_7H_8O \cdot 5H_2O$ by R_3 , and the dissociation of $\beta\text{-CD} \cdot C_7H_8O$ by D_2 mechanisms.

Non-isothermal studies

Figure 4 shows the TG and DTG heating curves. For a non-isothermal process

$$\frac{d\alpha}{dT} = \frac{A}{\beta} e^{-E/RT} f(\alpha) \quad (5)$$

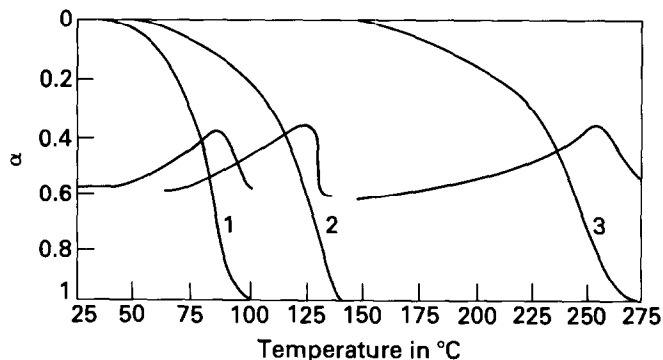


Fig. 4. TG and DTG curves, heating rate = $2.5^{\circ}\text{C min}^{-1}$: 1, dehydration of $\beta\text{-CD} \cdot \text{C}_7\text{H}_8\text{O} \cdot 5\text{H}_2\text{O}$; 2, evaporation of $\text{C}_7\text{H}_8\text{O}$; 3, dissociation of $\beta \cdot \text{CD} \cdot \text{C}_7\text{H}_8\text{O}$.

The integral form is

$$g(\alpha) = \frac{ART^2}{\beta E} \left[1 - \frac{2RT}{E} \right] e^{-E/RT} \quad (6)$$

where A is the pre-exponential factor of the Arrhenius equation, E is the activation energy, and β the heating rate, because $E \gg 2RT$. Combining eqns. (5) and (6), and rearranging

$$f(\alpha)g(\alpha) = T^2 \frac{d\alpha}{dt} \frac{R}{\beta E} \left[1 - \frac{2RT}{E} \right] \quad (7)$$

Let $\alpha = 0.5$

$$f(0.5)g(0.5) = T_{0.5}^2 \left(\frac{d\alpha}{dt} \right)_{0.5} \frac{R}{\beta E} \left[1 - \frac{2RT_{0.5}}{E} \right] \quad (8)$$

where $T_{0.5}$ is the temperature at $\alpha = 0.5$, and $(d\alpha/dt)_{0.5}$ is the rate of weight loss at $\alpha = 0.5$. From eqns. (7) and (8)

$$\frac{f(\alpha)g(\alpha)}{f(0.5)g(0.5)} = \left(\frac{T}{T_{0.5}} \right)^2 \frac{(d\alpha/dt)}{(d\alpha/dt)_{0.5}} \quad (9)$$

For a given mechanism function, the plot of $[f(\alpha)g(\alpha)]/[f(0.5)g(0.5)]$ versus α will give a standard curve and the plot of $(T/T_{0.5})^2[(d\alpha/dt)/(d\alpha/dt)_{0.5}]$ versus α will give an experimental curve. The suitable mechanism function can be defined by comparing the experimental and standard curves. Figure 5 shows the standard curves of various model functions, and indicates that the experimental points for benzyl alcohol and $\beta\text{-CD} \cdot \text{C}_7\text{H}_8\text{O} \cdot 5\text{H}_2\text{O}$ fit accurately the R_1 and R_3 mechanisms, respectively. The experimental points for the dissociation of $\beta\text{-CD} \cdot \text{C}_7\text{H}_8\text{O}$ fall on curve D_2 .

Combining isothermal and non-isothermal experiments, we come to the conclusion that the evaporation of $\text{C}_7\text{H}_8\text{O}$ is dominated by R_1 , the dehydration by R_3 , and the dissociation by D_2 mechanisms.

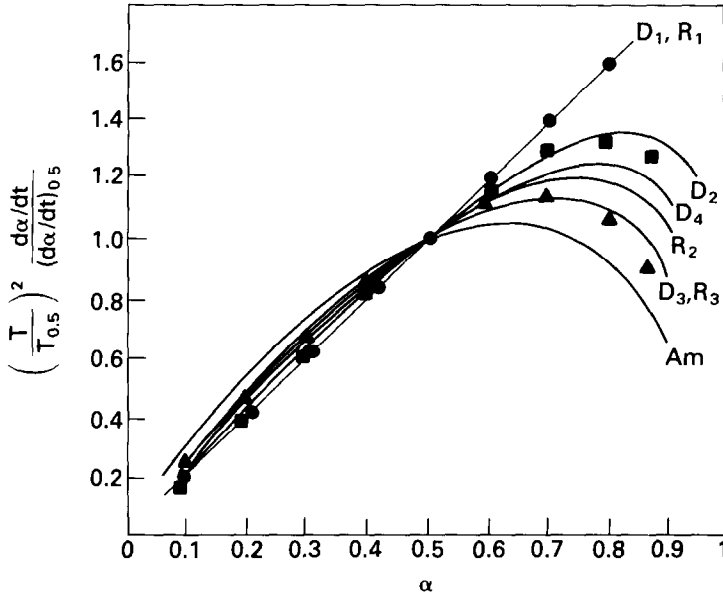


Fig. 5. Standard curves for ●, the evaporation of C_7H_8O ; ▲, the dehydration of $\beta\text{-CD} \cdot C_7H_8O \cdot 5H_2O$; ■, the dissociation of $\beta\text{-CD} \cdot C_7H_8O$.

Calculation of the kinetic parameters

Equation (6) can be converted into the form

$$\log \frac{g(\alpha)}{T^2} = \log \frac{AR}{\beta E} \left[1 - \frac{2RT}{E} \right] - \frac{E}{2.303R} \frac{1}{T} \quad (10)$$

Generally, because $E \gg 2RT$, E and A can be obtained from a linear regression fit of $\log[g(\alpha)/T^2]$ versus $1/T$.

It must be expressed that the parameters obtained by non-isothermal methods are different at different heating rates. This difference is due to a thermal lag phenomenon such that the temperature of the sample cannot catch up with the programmed temperature at high heating rates. The faster the heating rate, the more the deviation in sample temperature from the programmed temperature. In order to eliminate this temperature deviation, we calculated the E and A values at different heating rates, $\beta = 1.2, 2.5, 5, 10^\circ\text{C min}^{-1}$, and then extrapolated β to zero [13]. Thus E and A values at $\beta = 0$ were obtained, see Table 3.

Crystal structure analysis

The structure of $\beta\text{-CD} \cdot C_7H_8O \cdot 5H_2O$

X-ray diffraction analysis shows that the complex of $\beta\text{-CD}$ with benzyl alcohol forms a cage-type structure. The guest benzyl alcohol molecules are

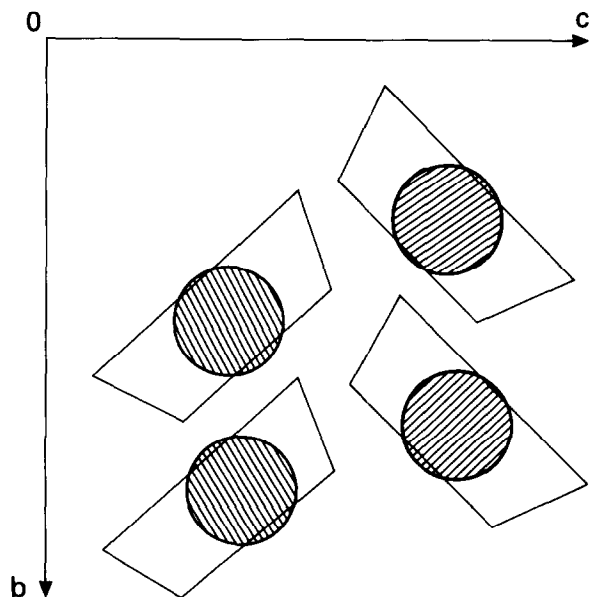
TABLE 3

The kinetic parameters at $\beta = 0$

Weight loss process	Mechanism	$E/\text{kJ mol}^{-1}$	A/min^{-1}	r
Evaporation of benzyl alcohol	R_1	41	1.972×10^3	0.9990
Dehydration of $\beta\text{-CD} \cdot \text{C}_7\text{H}_8\text{O} \cdot 5\text{H}_2\text{O}$	R_3	102	9.5×10^{10}	0.9990
Dissociation of $\beta\text{-CD} \cdot \text{C}_7\text{H}_8\text{O}$	D_2	158	3.262×10^{14}	0.9996

fully enclosed within the host cavity. Five water molecules are distributed in the intermolecular spaces between the $\beta\text{-CD}$ molecules. The crystal is monoclinic with the space group $P2_1$, $Z = 2$, $a = 15.4 \text{ \AA}$, $b = 10.1 \text{ \AA}$, $c = 20.9 \text{ \AA}$, and $\beta = 109.90^\circ$ [14]. The structure of $\beta\text{-CD} \cdot \text{C}_7\text{H}_8\text{O} \cdot 5\text{H}_2\text{O}$ is shown in Fig. 6.

Scanning electron microscopic observations indicate that the size and the formal structure of $\beta\text{-CD}$ obtained by heating $\beta\text{-CD} \cdot \text{C}_7\text{H}_8\text{O}$ and those of $\beta\text{-CD} \cdot \text{C}_7\text{H}_8\text{O}$ obtained by heating $\beta\text{-CD} \cdot \text{C}_7\text{H}_8\text{O} \cdot 5\text{H}_2\text{O}$ have no marked difference from those of $\beta\text{-CD} \cdot \text{C}_7\text{H}_8\text{O} \cdot 5\text{H}_2\text{O}$. For the dehydration and dissociation process, the crystals do not break into pieces, but deform to a small extent, see Fig. 7.

Fig. 6. Crystal structure of $\beta\text{-CD} \cdot \text{C}_7\text{H}_8\text{O} \cdot 5\text{H}_2\text{O}$ viewed along the a -axis.

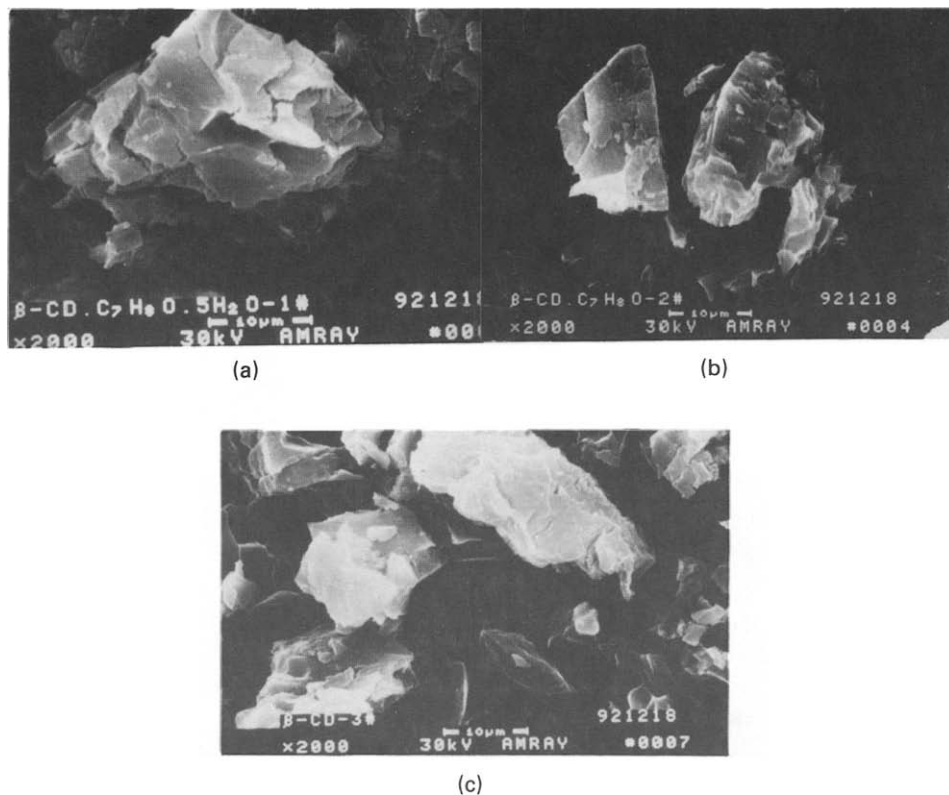


Fig. 7. Crystals of (a) $\beta\text{-CD} \cdot \text{C}_7\text{H}_8\text{O} \cdot 5\text{H}_2\text{O}$, (b) $\beta\text{-CD} \cdot \text{C}_7\text{H}_8\text{O}$, (c) $\beta\text{-CD}$.

The dehydration of $\beta\text{-CD} \cdot \text{C}_7\text{H}_8\text{O} \cdot 5\text{H}_2\text{O}$

The general kinetic pattern of the solid-state reaction can be divided into three stages [15]. In the first stage, individual crystal nuclei of the new phase are slowly formed on the surface (induction period, usually $\alpha < 0.05$). In stage two, the crystal nuclei grow and some individual crystals coalesce, producing a continuous layer of solid ($\alpha < 0.1$). In stage three, the phase interface moves towards the interior of the particles. Obviously, in stages one and two the reaction rate is dependent on the nucleation and growth. In stage three the reaction rate is dependent on the slowest step in the interface reaction; the gas molecules diffuse towards the surface and desorption occurs from the crystal surface. Our interest falls in the range of $\alpha = 0.1\text{--}0.9$, so only stage three is considered here.

In the dehydration of $\beta\text{-CD} \cdot \text{C}_7\text{H}_8\text{O} \cdot 5\text{H}_2\text{O}$, as the temperature increases, first the hydrogen bonds between the water molecules and $\beta\text{-CD}$ break, and further water molecules diffuse towards the crystal surface; finally the water desorbs from the surface. Because the water molecules are distributed in the intermolecular spaces between the $\beta\text{-CD}$ molecules and because the water molecules are small, the diffusion step is fast. When the

temperature exceeds 50°C, the desorption step is fast. The reaction rate is dependent on the rate of hydrogen bond breaking. Although the spacial stacking of β -CD · C₇H₈O along the various directions is different, due to their small volume the water molecules can diffuse in various directions. In other words, the reaction interface is three-dimensional. The results are consistent with an R₃ mechanism, as identified by the TG and DTG analyses.

The dissociation of β -CD · C₇H₈O

In the dissociation of β -CD · C₇H₈O, first the benzyl alcohol molecules escape from the β -CD cages, diffuse towards the crystal surface and finally desorb from the surface. It has been confirmed that the stable energy of inclusion complexes of β -CD with weakly polar guest molecules consists mainly of Van der Waals energy [16, 17]. The escape of the guest molecules from the β -CD cavity is easy. The dissociation temperature far exceeds the temperature of the evaporation of benzyl alcohol, and the desorption is fast. Because of the large volume of the benzyl alcohol molecule, diffusion is difficult compared with that of water. Therefore the diffusion step is rate-controlling for the dissociation of β -CD · C₇H₈O.

Due to crystal anisotropism, diffusion is different when the product gas moves towards different crystal surfaces. From Fig. 6, we can see that along the *b*-axis, the β -CD molecules are not cylindrical but cage-like. The β -CD molecules stack in the *bc*-plane forming a compact molecular layer. These layers arrange along the *a*-axis and form a sheet-like structure. This graphite-like structure can be clearly observed in Fig. 7. Thus benzyl alcohol molecules escaping from one β -CD cavity cannot easily get into another β -CD cage along the *b*-axis. It is also difficult to move along the *a*-axis because of the compact layer of molecules. So the benzyl alcohol molecules can move only towards the [010], [001] plane in the space between two layers of β -CD molecules. In other words, the diffusion of benzyl alcohol towards the surface is two-dimension, D₂.

CONCLUSIONS

β -CD can form a stable inclusion complex with volatile benzyl alcohol, β -CD · C₇H₈O · 5H₂O. The dehydration of β -CD · C₇H₈O is dominated by an R₃ mechanism. The dissociation of β -CD · C₇H₈O is dominated by a D₂ mechanism.

Thermogravimetric measurements can elucidate the dynamic processes of the thermal decomposition reaction. X-ray diffraction and scanning electron microscopy can determine the crystal structure of the sample and the product. Combining the TG, DTG, X-ray diffraction and microscopy results together provide a more clear understanding of the thermal decomposition processes.

REFERENCES

- 1 C. Betzel, W. Saenger, B.E. Hingerty and G.M. Brown, *J. Am. Chem. Soc.*, 106 (1984) 7545.
- 2 Z. Chongpu and Z. Yonggany, *Yaouxue Tongbao*, 22(2) (1987) 101.
- 3 D. Dominique and W. Denis, *Acta Pharm. Technol.*, 36 (1990) 1.
- 4 S.K. Samant and J.S. Pai, *Indian Food Packer*, 45(3) (1991) 55.
- 5 L. Szente, M. Gal-Fuzy and J. Szejtli, *Acta Aliment. Acad. Sci. Hung.*, 17(2) (1988) 193–9.
- 6 T. Tatsuyoshi, D. Toshio and S. Isao, *Bull. Chem. Soc. Jpn.*, 63(4) (1990) 1246–8.
- 7 J. Yanbao, H. Xianzhi and C. Guozhen, *Gaodeng Xuexiao Huaxue Xuebao*, 12(7) (1991) 961–4.
- 8 Y. Masuda, K. Iwata, R. Ito and Y. Ito, *J. Phys. Chem.*, 91 (1987) 6543–6547.
- 9 Y. Masuda and K. Nagagata, *Thermochim. Acta*, 161 (1990) 55–60.
- 10 M. Ben-Amor, J.C. Mutin, A. Aubry and A. Courtois, *J. Solid State Chem.*, 48 (1983) 215–230.
- 11 J.H. Sharp, G.W. Brindey and B.N. Narahaki, *J. Am. Ceram. Soc.*, 379 (1966) 49.
- 12 J.M. Criado, *Thermochim. Acta*, 24 (1978) 186.
- 13 L. Jinghua, Z. Guien and H. Shan, *Gaodeng Xuexiao Huaxue Xuebao*, 12(11) (1991) 1513.
- 14 K. Harata, K. Uekama, M. Otagiri, F. Hirayama and Y. Ohtani, *Bull. Chem. Soc. Jpn.*, 58 (1985) 1234.
- 15 L. Jinghua, Z. Guien and L. Wen, *Thermochim. Acta.*, 205 (1992) 145–156.
- 16 M. Ohashi, K. Kasatami, H. Shinohara and H. Sato, *J. Am. Chem. Soc.*, 112 (1990) 5824.
- 17 L. Tianxiong, Z. Dongbo and D. Shaojun, *J. Chem. Soc. Faraday Trans. 2*, 85 (1989) 1439.